ANISOTROPY OF EFFECTIVE MASSES OF HOLES IN LEAD

K. Sh. AGABABYAN, R. T. MINA, and V. S. POGOSYAN

Erevan Physics Institute

Submitted August 31, 1967

Zh. Eksp. Teor. Fiz. 54, 721–726 (March, 1968)

Effective masses corresponding to orbits on the hole Fermi surface of lead of the 1-OPW model are calculated with the aid of an electronic computer and their anisotropy is found in the crystallographic (001) and (011) surfaces. The results of the calculation are compared with the experimental data of [4]. The position of the orbits of two non-central cyclotron resonances, the origin of which had been unknown, is determined. It is shown that a good agreement between the calculated and experimental effective masses is a consequence of an approximately identical distribution of the rates of holes on the 1-OPW surface and on the real Fermi surface of lead.

EXPERIMENTS [1-5] aimed at studying the Fermi surface of lead have shown convincingly that the latter is close to the model of almost free electrons, constructed in the 1-OPW approximation [1,6]. In accordance with this model, the Fermi surface of lead is made up of a closed hole surface (Fig. 1) and multiply connected electron surface.

At the same time, the same experiments revealed quantitative differences from the simple 1-OPW model. A more perfect model, constructed by Anderson and Gold in the 4-OPW approximation [5], with allowance of the spin-orbit coupling of the conduction electrons, was in better agreement with the experimental results. The periods of the de Haas–van Alphen oscillations calculated in accordance with this model, and their anisotropy, practically coincided with those observed in the experiment. This offers evidence that the form of the 4-OPW model of the Fermi surface is quite close to the real one.

A comparison, made by Anderson and Gold [5], of the values of the effective masses measured in [3,4] and calculated in accordance with the 4-OPW model, has shown that for different orbits the experimental values exceed by approximately two times the calculated ones. This difference is attributed [7,8] to the existence of a considerable electron-phonon interaction in lead, as confirmed by its superconductivity [8,9]. Owing to this interaction, the carrier velocities decrease, leading to an increase in the time of their revolution over the orbit, i.e., to an increase of the observed effective mass. The fact that for entirely different orbits the effective mass is approximately two times larger (accurate to 10–15%) from that calculated with the 4-OPW model offers evidence of an approximate isotropy of the electron-photon interaction.

One of the authors and Khaĭkin [4] observed in lead a considerable number of cyclotron resonances, many of which were interpreted qualitatively. In the present paper we calculate the effective masses of the holes and present a comparison with the experimental data of [4], as a result of which we are able to identify certain noncentral cyclotron resonances. In view of definite computational difficulties, we chose the 1-OPW model of the hole Fermi surface. The basis for such a choice was also the fact that for the large hole Fermi surface in lead the effective mass calculated for the models 1-OPW and 4-OPW differ insignificantly, by approximately 2–3%. This is confirmed both by direct calculations for certain cyclotron resonances (Table IV in [5]), and by the arguments presented in [10]. A noticeable difference occurs only if the plane of the orbit is close to the Brillouin plane. For example, this takes for a central orbit at $\mathbf{H} \parallel [100]$. But even in this case the difference does not exceed 15%.

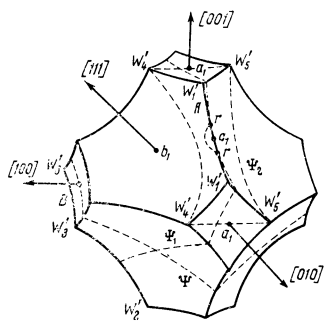

FIG. 1. Hole Fermi surface of lead in accordance with the 1-OPW model. The letters Ψ, Ψ_1, and Ψ_2 denote respectively the central and the two non-central orbits. The positions of the orbits are as follows: Ψ – $\mathbf{H} \parallel [011]$, $p_H = 0$; $\sphericalangle(\mathbf{H}, [100]) = 30°$ in the (011) plane, $p_H = 0.35$ h/a; Ψ_2 – $\mathbf{H} \parallel [011]$, $p_H = 0.56$ h/a. The remaining letters indicate the surface elements that are symmetrical with respect to the (011) plane.

CALCULATION OF EFFECTIVE MASSES OF HOLES

The tetravalent metal lead has a face-centered cubic lattice. Its hole Fermi surface in the 1-OPW model (Fig. 1) is formed by intersection of 14 Fermi spheres of radius $p_S = 1.24$ h/a, the centers of which are located in the nearest sites of the body-centered cubic reciprocal lattice [1,6]. In a magnetic field, the orbit of the hole in momentum space is the intersection of this surface with the plane perpendicular to the direction of the magnetic field. Different sections of the Fermi surface differ in the corresponding values of the momentum component p_H of the hole in the direction of the magnetic field.

As shown in [4], calculation of the effective mass in accordance with the 1-OPW model reduces to a determination of the sum of the angular dimensions φ_n of the arcs, of which the orbit is made up, using the formula

$$\mu_0 = \frac{\mu_e}{2\pi} \sum_n \varphi_n,$$

where $\mu_S = p_S/v_S m_e$ is the relative effective mass of

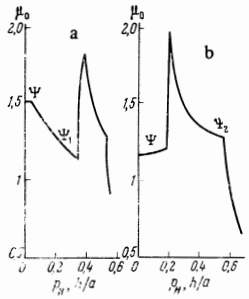

FIG. 2. Plot of the calculated effective mass μ_0 vs. momentum projection p_H for two directions of the magnetic field: a – $\sphericalangle$ (H, [100]) = 30° in the (0$\bar{1}$1) plane, b – H ∥ [011].

the carrier moving with velocity v_S on a Fermi sphere of radius p_S.

The calculation, a detailed description of which will be published later, was made with the "Razdan-2" electronic computer for the crystallographic plane (001) in the angle interval 0–45° and for the plane (0$\bar{1}$1) in the angle interval 0–90° in steps of 2.5°. For each value of the angle we found the effective masses μ_0 corresponding to the intersections of the hole surface with parallel planes in steps of $\Delta p_H = 0.01$ h/a in the interval $0 \le p_H \le 0.6$ h/a. The calculation data were used to plot μ_0 against p_H, similar to that shown in Fig. 2. On the basis of a comparison made by Anderson and Gold in [5], it was assumed here that $\mu_S = 2$.

A characteristic of such plots is the rapid growth of the effective mass μ_0 occurring at definite values of p_H (for example, at $p_H = 0.35$ on Fig. 2a), or a rapid decrease of the effective mass (for example, at $p_H = 0.56$ on Fig. 2b).

The first of these singularities appears whenever the plane of the orbit crosses twice the edge of the Fermi surface between neighboring vertices. For example, on Fig. 1 the plane of the orbit Ψ_1 at the point r crosses the edge A between the vertices W_1'. The same orbit is shown in Fig. 3, together with another one, constructed at a close value of p_H. The plane of one of them does not cross the edge, and that of the other crosses. It is seen that when p_H changes only by 0.01 h/a, the angular dimension of the orbit increases rapidly as a result of the appearance of a new arc with appreciable angular dimension. If the effective mass decreases with increasing p_H prior to the appearance of this singularity, a minimum of the effective mass is produced at the kink. This leads to the appearance of cyclotron resonance on an orbit whose plane is "tied" to the point on the edge of the Fermi surface. For example, when the angle between H, and [100] lies between 0° and 42° in the (0$\bar{1}$1) plane the orbit Ψ_1 passes through the point c_1 (Fig. 1).

The second of the singularities of the $\mu_0(p_H)$ plots, namely the sharp decrease of the effective mass (Fig. 2b), occurs at sufficiently large values of p_H, when the angular dimensions of all the arcs making up the orbit, starting with a definite value of p_H (for example, $p_H = 0.56$ on Fig. 2b), decrease simultaneously. This leads to a sharp kink in the $\mu_0(p_H)$ plot at the indicated value of p_H. In the case under consideration, a noncentral extremal orbit Ψ_2, on which cyclotron resonances are possible, occurs ahead of the kink.

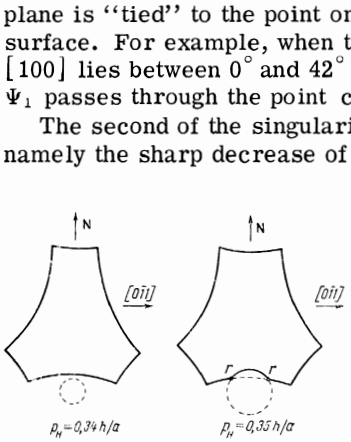

FIG. 3. Hole orbits for close values of p_H at $\sphericalangle$ (H, [100]) = 30° in the (011) plane. One of them is shown in Fig. 1. The dashed lines show the sections of the Fermi spheres emerging beyond the limits of the hole surface

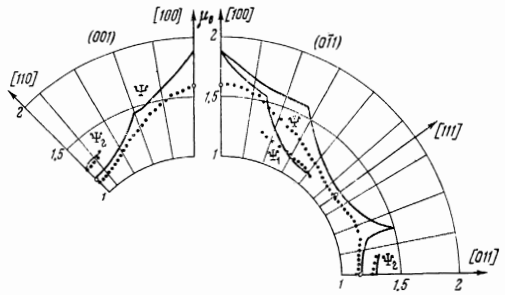

FIG. 4. Anisotropy of the hole effective masses in lead in two crystallographic planes, (0$\bar{1}$1) and (001). The solid lines show the results of calculations in accordance with the 1-OPW model; ○ – calculation by the 4-OPW model [5], ○ – experimental data of [14].

The angle diagrams of Fig. 4 show the extremal effective masses obtained from plots similar to those shown in Fig. 2. The effective masses for rational directions of the magnetic field are as follows:

$$\mu_{\Psi[011]} = 0.58\,\mu_s, \quad \mu_{\Psi[111]} = 0.60\,\mu_s, \quad \mu_{\Psi[100]} = 0.94\,\mu_s.$$

The first two values coincide with the values given in Table IV of [5].

The value $\mu_\Psi[100] = 0.668\,\mu_S$ given by Anderson and Gold [5] is wrong, apparently as a result of an incorrect calculation. Indeed, the carrier velocity in the 1-OPW model is constant throughout and is equal to $v_S = 1.24\,(h/a)/\mu_S m_e$, with the exception of its edges, where, as shown in [10], the velocity is equal in magnitude to the projection of the carrier velocity, at a point arbitrarily close to the edge, on the plane of the edge, and lies in this plane. When H ∥ [100], the central orbit Ψ passes over four edges of the hole surface (Fig. 1). If it is assumed erroneously in the calculation of $\mu_\Psi[100]$ that $\hat{v}_S = v_S$, then the calculation yields $\mu_\Psi[100] = 0.67$, which is the value given in [5].

The text of [4] gives the incorrect value $\mu_\Psi[111] = 0.77\,\mu_S$. On the other hand, the anisotropy of the calculated mass Ψ, shown in Fig. 4 of [4], agrees well with the results of the present calculation.

COMPARISON OF CALCULATION RESULTS WITH THE EXPERIMENTAL DATA

A comparison of the results of the present work with experiments performed in [4] shows that satisfactory quantitative agreement, for both the absolute values of μ and for the angle intervals of their existence, occurs for three effective masses Ψ, Ψ_1, and Ψ_2. The latter, the value of which lies between the masses Ψ and χ, is not designated in [4], since no particular orbit has been identified with it. The anisotropy of the effective masses Ψ, Ψ_1, and Ψ_2 and the calculated plots ascribed to them are shown in Fig. 4.

CENTRAL HOLE ORBIT Ψ

Figure 4 shows three double values of μ, calculated by Anderson and Gold[5], for the central hole orbit in accordance with the 4-OPW model, with the magnetic field **H** directed along the axes [100], [111], and [011]. The fact that these values are practically equal to the measured ones shows that the entire difference between calculations in accordance with the 1-OPW model and the experimentally determined anisotropic mass is due to the decrease of the dimensions of the Fermi surface (Figs. 9 and 10 in[5]) and the change in the carrier velocities on the surface.

These changes are most significant near the edges of the Fermi surface. Therefore, when the orbit passes over the edges and its plane is close to the Brillouin plane in which these edges lie, the effective mass corresponding to such an orbit differs noticeably from that calculated in accordance with the 1-OPW model. Indeed, when **H** ∥ [011] the central orbit Ψ crosses orthogonally the six edges of the surface, when **H** ∥ [111] the six edges are crossed at an angle 55°, and when the angle between **H** and [011] equals 16° in the $(0\bar{1}1)$ plane the central orbit passes over two edges at an angle 15°, and finally when **H** ∥ [100] the central orbit lies in the Brillouin plane and passes over four edges of the surface. It is seen from Fig. 4 how the agreement with calculation in accordance with the 1-OPW model deteriorates gradually for these cases.

NONCENTRAL HOLE ORBITS Ψ_1 AND Ψ_2

The position of the noncentral orbits Ψ_1, shown in Fig. 1, is such that its plane passes through the center of the edge A at the point c_1. Therefore the interval of existence of the orbit Ψ_1, equal to 28° (Fig. 4), is determined by its two extreme positions, at which the orbit falls on the vertices W_2' and W_3' of the hole surface. The passage of the orbit through the vertices W_2' upon rotation of the direction of the magnetic field corresponds to a kink on the plot of the effective mass Ψ_1 on Fig. 4 when the angle between **H** and [100] is 14°, and passage through the vertex W_3' corresponds to vanishing of cyclotron resonance in view of the abrupt change in the value of the effective mass, which occurs when the edge B is crossed twice (Fig. 1). The monotonic decrease of μ_{Ψ_1}, compared with the calculated value as the magnetic field direction is rotated towards the [100] axis, is connected with the approach of the plane of the orbit to the Brillouin plane (001) in which the edge A lies. In this case there is a complete analogy with the behavior of the effective mass of the central cyclotron resonance Ψ.

The effective mass Ψ_2 is quantitatively in good agreement with the calculated value for the orbit Ψ_2, shown in Fig. 1. The existence of this resonance is connected with the presence of a sharp kink on the $\mu_0(p_H)$ plot, when the orbit Ψ_1 passes simultaneously over the four vertices W_4' and W_5' of the hole surface at **H** ∥ [011] (Fig. 1). When the direction of the magnetic field is rotated away from the [011] axis, the interval of p_H in which the vertices W_4' and W_5' pass in succession increases, the kink on the $\mu_0(p_H)$ plot (Fig. 2b) spreads out, and the cyclotron resonance ceases to exist. It is seen from Fig. 4 that the angle interval in which the resonance Ψ_2 exists agrees well with the calculated one in both crystallographic planes $(0\bar{1}1)$ and (001).

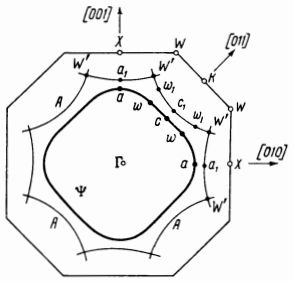

FIG. 5. Central section of the Brillouin zone of the hole surface of the 1-OPW and 4-OPW models in the (001) plane [5]. The letters a, w, and c (a_1, w_1, and c_1) indicate the points lying at the intersections of the rays ΓX, ΓW, and ΓK with the hole surface of the 4-OPW model (1-OPW model); the letters W′ and A denote the vertices and the edges of the hole surface in the 1-OPW model.

DISCUSSIONS

The foregoing comparison has shown the suitability of the 1-OPW model for the interpretation of cyclotron resonances in lead. At first glance this seems surprising, since the real hole Fermi surface, to which the 4-OPW model is closer, differs greatly in shape from the simple 1-OPW model. It is seen clearly from Fig. 5, which shows the cross sections for the hole surface of these two models, that the edge A on the 4-OPW model becomes convex, and the vertices W′ are missing. Nonetheless, those singularities of the shape of the surface, which are present in the 1-OPW model and absent from the smoother 4-OPW model, become manifest, although in weaker form, in the anisotropy of the effective masses. This can be verified by tracing, for example, the behavior of the effective mass Ψ in the interval 0—35° of the angle between **H** and [011] in the $(0\bar{1}1)$ plane on Fig. 4. The cyclotron resonance "senses" when the orbit passes over the nonexistent "vertices" and the edge between them. The appearance of the "vanished" properties of the 1-OPW model is due to the fact that the carrier velocity distribution on the Fermi surface, which determines to a considerable degree the magnitude of the effective mass, is approximately the same in both models.

The table lists the velocities of the holes at four different points (with allowance for symmetry in 8 + 6 + 24 + 12 = 50 points) of the hole surface for the 1-OPW and 4-OPW models. The accuracy indicated in the table corresponds not to Anderson and Gold's calculations themselves[5], but to the determination of these quantities from Fig. 11 of their paper. It follows from the table that when the velocities on the hole surface change by approximately 1.7 times, the difference for the two models does not exceed several per cent.

1-OPW model		4-OPW model		Direction to point (Fig. 5)
Point on Fig. 5	Hole velocity*	Point on Fig. 5	Hole velocity*	
b_1**	1.24	b***	1,24±0,05	ΓL
a_1	1.24	a	1,06±0,04	ΓX
w_1	0.73	w	0,80±0,03	ΓW
c_1	0.73	c	0,78±0,03	ΓK

*The hole velocity is given in units of $(h/a)/\mu_s m_e$.
**Point on Fig. 1.
***Point on Fig. 9 in [5].

In conclusion, the authors consider it their pleasant duty to thank A. I. Alikhanyan for interest in the work, M. S. Khaikin for useful discussions and remarks, and M. E. Arustamov for great help with the calculations.

[1] A. V. Gold, Phil. Trans. Roy. Soc. London A251, 85 (1958).

[2] N. E. Alekseevskiĭ and Yu. P. Gaidukov, Zh. Eksp. Teor. Fiz. 41, 354 (1961) [Sov. Phys.-JETP 14, 256 (1962)]. J. E. Schirber, Phys. Rev. 131, 2459 (1963).

[3] R. C. Young, Phil. Mag. 7, 2065 (1962).

[4] R. T. Mina and M. S. Khaĭkin, Zh. Eksp. Teor. Fiz. 45, 1304 (1963) [Sov. Phys.-JETP 18, 896 (1964)].

[5] J. R. Anderson and A. V. Gold. Phys. Rev. 139A, 1459 (1965).

[6] W. A. Harrison, Phys. Rev. 118, 1190 (1960).

[7] S. N. Nakajima and M. Vatabe, Progr. Theor. Phys. 30, 772 (1962).

[8] J. S. Swihart, D. J. Scalapino, and J. Wada, Phys. Rev. Lett. 14, 106 (1965).

[9] W. J. Tomash and T. Wolfram, Phys. Rev. Lett. 16, 952 (1966).

[10] R. T. Mina and M. S. Khaĭkin, Zh. Eksp. Teor. Fiz. 51, 62 (1966) [Sov. Phys.-JETP 24, 42 (1967)].

Translated by J. G. Adashko
106